

A Structure at 2175 MeV in $e^+e^- \rightarrow \phi f_0(980)$ Observed via Initial-State Radiation

B. Aubert,¹ M. Bona,¹ D. Boutigny,¹ F. Couderc,¹ Y. Karyotakis,¹ J. P. Lees,¹ V. Poireau,¹ V. Tisserand,¹
A. Zghiche,¹ E. Grauges,² A. Palano,³ J. C. Chen,⁴ N. D. Qi,⁴ G. Rong,⁴ P. Wang,⁴ Y. S. Zhu,⁴ G. Eigen,⁵
I. Ofte,⁵ B. Stugu,⁵ G. S. Abrams,⁶ M. Battaglia,⁶ D. N. Brown,⁶ J. Button-Shafer,⁶ R. N. Cahn,⁶ E. Charles,⁶
M. S. Gill,⁶ Y. Groyzman,⁶ R. G. Jacobsen,⁶ J. A. Kadyk,⁶ L. T. Kerth,⁶ Yu. G. Kolomensky,⁶ G. Kukartsev,⁶
G. Lynch,⁶ L. M. Mir,⁶ T. J. Orimoto,⁶ M. Pripstein,⁶ N. A. Roe,⁶ M. T. Ronan,⁶ W. A. Wenzel,⁶ P. del
Amo Sanchez,⁷ M. Barrett,⁷ K. E. Ford,⁷ T. J. Harrison,⁷ A. J. Hart,⁷ C. M. Hawkes,⁷ A. T. Watson,⁷
T. Held,⁸ H. Koch,⁸ B. Lewandowski,⁸ M. Pelizaeus,⁸ K. Peters,⁸ T. Schroeder,⁸ M. Steinke,⁸ J. T. Boyd,⁹
J. P. Burke,⁹ W. N. Cottingham,⁹ D. Walker,⁹ D. J. Asgeirsson,¹⁰ T. Cuhadar-Donszelmann,¹⁰ B. G. Fulsom,¹⁰
C. Hearty,¹⁰ N. S. Knecht,¹⁰ T. S. Mattison,¹⁰ J. A. McKenna,¹⁰ A. Khan,¹¹ P. Kyberd,¹¹ M. Saleem,¹¹
D. J. Sherwood,¹¹ L. Teodorescu,¹¹ V. E. Blinov,¹² A. D. Bukin,¹² V. P. Druzhinin,¹² V. B. Golubev,¹²
A. P. Onuchin,¹² S. I. Serednyakov,¹² Yu. I. Skovpen,¹² E. P. Solodov,¹² K. Yu Todyshev,¹² M. Bondioli,¹³
M. Bruinsma,¹³ M. Chao,¹³ S. Curry,¹³ I. Eschrich,¹³ D. Kirkby,¹³ A. J. Lankford,¹³ P. Lund,¹³ M. Mandelkern,¹³
R. K. Mommsen,¹³ W. Roethel,¹³ D. P. Stoker,¹³ S. Abachi,¹⁴ C. Buchanan,¹⁴ S. D. Foulkes,¹⁵ J. W. Gary,¹⁵
O. Long,¹⁵ B. C. Shen,¹⁵ K. Wang,¹⁵ L. Zhang,¹⁵ H. K. Hadavand,¹⁶ E. J. Hill,¹⁶ H. P. Paar,¹⁶ S. Rahatlou,¹⁶
V. Sharma,¹⁶ J. W. Berryhill,¹⁷ C. Campagnari,¹⁷ A. Cunha,¹⁷ B. Dahmes,¹⁷ T. M. Hong,¹⁷ D. Kovalskyi,¹⁷
J. D. Richman,¹⁷ T. W. Beck,¹⁸ A. M. Eisner,¹⁸ C. J. Flacco,¹⁸ C. A. Heusch,¹⁸ J. Kroseberg,¹⁸ W. S. Lockman,¹⁸
G. Nesom,¹⁸ T. Schalk,¹⁸ B. A. Schumm,¹⁸ A. Seiden,¹⁸ P. Spradlin,¹⁸ D. C. Williams,¹⁸ M. G. Wilson,¹⁸
J. Albert,¹⁹ E. Chen,¹⁹ A. Dvoretzkii,¹⁹ F. Fang,¹⁹ D. G. Hitlin,¹⁹ I. Narsky,¹⁹ T. Piatenko,¹⁹ F. C. Porter,¹⁹
A. Ryd,¹⁹ G. Mancinelli,²⁰ B. T. Meadows,²⁰ K. Mishra,²⁰ M. D. Sokoloff,²⁰ F. Blanc,²¹ P. C. Bloom,²¹ S. Chen,²¹
W. T. Ford,²¹ J. F. Hirschauer,²¹ A. Kreisel,²¹ M. Nagel,²¹ U. Nauenberg,²¹ A. Olivas,²¹ W. O. Ruddick,²¹
J. G. Smith,²¹ K. A. Ulmer,²¹ S. R. Wagner,²¹ J. Zhang,²¹ A. Chen,²² E. A. Eckhart,²² A. Soffer,²² W. H. Toki,²²
R. J. Wilson,²² F. Winklmeier,²² Q. Zeng,²² D. D. Altenburg,²³ E. Feltresi,²³ A. Hauke,²³ H. Jasper,²³ J. Merkel,²³
A. Petzold,²³ B. Spaan,²³ T. Brandt,²⁴ V. Klose,²⁴ H. M. Lacker,²⁴ W. F. Mader,²⁴ R. Nogowski,²⁴ J. Schubert,²⁴
K. R. Schubert,²⁴ R. Schwierz,²⁴ J. E. Sundermann,²⁴ A. Volk,²⁴ D. Bernard,²⁵ G. R. Bonneaud,²⁵ E. Latour,²⁵
Ch. Thiebaux,²⁵ M. Verderi,²⁵ P. J. Clark,²⁶ W. Gradl,²⁶ F. Muheim,²⁶ S. Playfer,²⁶ A. I. Robertson,²⁶ Y. Xie,²⁶
M. Andreotti,²⁷ D. Bettoni,²⁷ C. Bozzi,²⁷ R. Calabrese,²⁷ G. Cibinetto,²⁷ E. Luppi,²⁷ M. Negrini,²⁷ A. Petrella,²⁷
L. Piemontese,²⁷ E. Prencipe,²⁷ F. Anulli,²⁸ R. Baldini-Ferrolli,²⁸ A. Calcaterra,²⁸ R. de Sangro,²⁸ G. Finocchiaro,²⁸
S. Pacetti,²⁸ P. Patteri,²⁸ I. M. Peruzzi,²⁸ * M. Piccolo,²⁸ M. Rama,²⁸ A. Zallo,²⁸ A. Buzzo,²⁹ R. Contri,²⁹ M. Lo
Vetere,²⁹ M. M. Macri,²⁹ M. R. Monge,²⁹ S. Passaggio,²⁹ C. Patrignani,²⁹ E. Robutti,²⁹ A. Santroni,²⁹ S. Tosi,²⁹
G. Brandenburg,³⁰ K. S. Chaisanguanthum,³⁰ M. Morii,³⁰ J. Wu,³⁰ R. S. Dubitzky,³¹ J. Marks,³¹ S. Schenk,³¹
U. Uwer,³¹ D. J. Bard,³² W. Bhimji,³² D. A. Bowerman,³² P. D. Dauncey,³² U. Egede,³² R. L. Flack,³²
J. A. Nash,³² M. B. Nikolich,³² W. Panduro Vazquez,³² P. K. Behera,³³ X. Chai,³³ M. J. Charles,³³ U. Mallik,³³
N. T. Meyer,³³ V. Ziegler,³³ J. Cochran,³⁴ H. B. Crawley,³⁴ L. Dong,³⁴ V. Eyges,³⁴ W. T. Meyer,³⁴ S. Prell,³⁴
E. I. Rosenberg,³⁴ A. E. Rubin,³⁴ A. V. Gritsan,³⁵ A. G. Denig,³⁶ M. Fritsch,³⁶ G. Schott,³⁶ N. Arnaud,³⁷
M. Davier,³⁷ G. Grosdidier,³⁷ A. Höcker,³⁷ F. Le Diberder,³⁷ V. Lepeltier,³⁷ A. M. Lutz,³⁷ A. Oyanguren,³⁷
S. Pruvot,³⁷ S. Rodier,³⁷ P. Roudeau,³⁷ M. H. Schune,³⁷ A. Stocchi,³⁷ W. F. Wang,³⁷ G. Wormser,³⁷ C. H. Cheng,³⁸
D. J. Lange,³⁸ D. M. Wright,³⁸ C. A. Chavez,³⁹ I. J. Forster,³⁹ J. R. Fry,³⁹ E. Gabathuler,³⁹ R. Gamet,³⁹
K. A. George,³⁹ D. E. Hutchcroft,³⁹ D. J. Payne,³⁹ K. C. Schofield,³⁹ C. Touramanis,³⁹ A. J. Bevan,⁴⁰
F. Di Lodovico,⁴⁰ W. Menges,⁴⁰ R. Sacco,⁴⁰ G. Cowan,⁴¹ H. U. Flaecher,⁴¹ D. A. Hopkins,⁴¹ P. S. Jackson,⁴¹
T. R. McMahan,⁴¹ S. Ricciardi,⁴¹ F. Salvatore,⁴¹ A. C. Wren,⁴¹ D. N. Brown,⁴² C. L. Davis,⁴² J. Allison,⁴³
N. R. Barlow,⁴³ R. J. Barlow,⁴³ Y. M. Chia,⁴³ C. L. Edgar,⁴³ G. D. Lafferty,⁴³ M. T. Naisbit,⁴³ J. C. Williams,⁴³
J. I. Yi,⁴³ C. Chen,⁴⁴ W. D. Hulsbergen,⁴⁴ A. Jawahery,⁴⁴ C. K. Lae,⁴⁴ D. A. Roberts,⁴⁴ G. Simi,⁴⁴ G. Blaylock,⁴⁵
C. Dallapiccola,⁴⁵ S. S. Hertzbach,⁴⁵ X. Li,⁴⁵ T. B. Moore,⁴⁵ S. Saremi,⁴⁵ H. Staengle,⁴⁵ R. Cowan,⁴⁶ G. Sciolla,⁴⁶
S. J. Sekula,⁴⁶ M. Spitznagel,⁴⁶ F. Taylor,⁴⁶ R. K. Yamamoto,⁴⁶ H. Kim,⁴⁷ S. E. McLaughlin,⁴⁷ P. M. Patel,⁴⁷
S. H. Robertson,⁴⁷ A. Lazzaro,⁴⁸ V. Lombardo,⁴⁸ F. Palombo,⁴⁸ J. M. Bauer,⁴⁹ L. Cremaldi,⁴⁹ V. Eschenburg,⁴⁹
R. Godang,⁴⁹ R. Kroeger,⁴⁹ D. A. Sanders,⁴⁹ D. J. Summers,⁴⁹ H. W. Zhao,⁴⁹ S. Brunet,⁵⁰ D. Côté,⁵⁰ M. Simard,⁵⁰
P. Taras,⁵⁰ F. B. Viaud,⁵⁰ H. Nicholson,⁵¹ N. Cavallo,⁵² † G. De Nardo,⁵² F. Fabozzi,⁵² † C. Gatto,⁵² L. Lista,⁵²

D. Monorchio,⁵² P. Paolucci,⁵² D. Piccolo,⁵² C. Sciacca,⁵² M. A. Baak,⁵³ G. Raven,⁵³ H. L. Snoek,⁵³ C. P. Jessop,⁵⁴ J. M. LoSecco,⁵⁴ T. Allmendinger,⁵⁵ G. Benelli,⁵⁵ L. A. Corwin,⁵⁵ K. K. Gan,⁵⁵ K. Honscheid,⁵⁵ D. Hufnagel,⁵⁵ P. D. Jackson,⁵⁵ H. Kagan,⁵⁵ R. Kass,⁵⁵ A. M. Rahimi,⁵⁵ J. J. Regensburger,⁵⁵ R. Ter-Antonyan,⁵⁵ Q. K. Wong,⁵⁵ N. L. Blount,⁵⁶ J. Brau,⁵⁶ R. Frey,⁵⁶ O. Igonkina,⁵⁶ J. A. Kolb,⁵⁶ M. Lu,⁵⁶ R. Rahmat,⁵⁶ N. B. Sinev,⁵⁶ D. Strom,⁵⁶ J. Strube,⁵⁶ E. Torrence,⁵⁶ A. Gaz,⁵⁷ M. Margoni,⁵⁷ M. Morandin,⁵⁷ A. Pompili,⁵⁷ M. Posocco,⁵⁷ M. Rotondo,⁵⁷ F. Simonetto,⁵⁷ R. Stroili,⁵⁷ C. Voci,⁵⁷ M. Benayoun,⁵⁸ H. Briand,⁵⁸ J. Chauveau,⁵⁸ P. David,⁵⁸ L. Del Buono,⁵⁸ Ch. de la Vaissière,⁵⁸ O. Hamon,⁵⁸ B. L. Hartfiel,⁵⁸ Ph. Leruste,⁵⁸ J. Malclès,⁵⁸ J. Ocariz,⁵⁸ L. Roos,⁵⁸ G. Therin,⁵⁸ L. Gladney,⁵⁹ M. Biasini,⁶⁰ R. Covarelli,⁶⁰ C. Angelini,⁶¹ G. Batignani,⁶¹ S. Bettarini,⁶¹ F. Bucci,⁶¹ G. Calderini,⁶¹ M. Carpinelli,⁶¹ R. Cenci,⁶¹ F. Forti,⁶¹ M. A. Giorgi,⁶¹ A. Lusiani,⁶¹ G. Marchiori,⁶¹ M. A. Mazur,⁶¹ M. Morganti,⁶¹ N. Neri,⁶¹ E. Paoloni,⁶¹ G. Rizzo,⁶¹ J. J. Walsh,⁶¹ M. Haire,⁶² D. Judd,⁶² D. E. Wagoner,⁶² J. Biesiada,⁶³ N. Danielson,⁶³ P. Elmer,⁶³ Y. P. Lau,⁶³ C. Lu,⁶³ J. Olsen,⁶³ A. J. S. Smith,⁶³ A. V. Telnov,⁶³ F. Bellini,⁶⁴ G. Cavoto,⁶⁴ A. D’Orazio,⁶⁴ D. del Re,⁶⁴ E. Di Marco,⁶⁴ R. Faccini,⁶⁴ F. Ferrarotto,⁶⁴ F. Ferroni,⁶⁴ M. Gaspero,⁶⁴ L. Li Gioi,⁶⁴ M. A. Mazzoni,⁶⁴ S. Morganti,⁶⁴ G. Piredda,⁶⁴ F. Polci,⁶⁴ F. Safai Tehrani,⁶⁴ C. Voena,⁶⁴ M. Ebert,⁶⁵ H. Schröder,⁶⁵ R. Waldi,⁶⁵ T. Adye,⁶⁶ N. De Groot,⁶⁶ B. Franek,⁶⁶ E. O. Olaiya,⁶⁶ F. F. Wilson,⁶⁶ R. Aleksan,⁶⁷ S. Emery,⁶⁷ A. Gaidot,⁶⁷ S. F. Ganzhur,⁶⁷ G. Hamel de Monchenault,⁶⁷ W. Kozanecki,⁶⁷ M. Legendre,⁶⁷ G. Vasseur,⁶⁷ Ch. Yèche,⁶⁷ M. Zito,⁶⁷ X. R. Chen,⁶⁸ H. Liu,⁶⁸ W. Park,⁶⁸ M. V. Purohit,⁶⁸ J. R. Wilson,⁶⁸ M. T. Allen,⁶⁹ D. Aston,⁶⁹ R. Bartoldus,⁶⁹ P. Bechtel,⁶⁹ N. Berger,⁶⁹ R. Claus,⁶⁹ J. P. Coleman,⁶⁹ M. R. Convery,⁶⁹ M. Cristinziani,⁶⁹ J. C. Dingfelder,⁶⁹ J. Dorfan,⁶⁹ G. P. Dubois-Felsmann,⁶⁹ D. Dujmic,⁶⁹ W. Dunwoodie,⁶⁹ R. C. Field,⁶⁹ T. Glanzman,⁶⁹ S. J. Gowdy,⁶⁹ M. T. Graham,⁶⁹ P. Grenier,⁶⁹ V. Halyo,⁶⁹ C. Hast,⁶⁹ T. Hryn’ova,⁶⁹ W. R. Innes,⁶⁹ M. H. Kelsey,⁶⁹ P. Kim,⁶⁹ D. W. G. S. Leith,⁶⁹ S. Li,⁶⁹ S. Luitz,⁶⁹ V. Luth,⁶⁹ H. L. Lynch,⁶⁹ D. B. MacFarlane,⁶⁹ H. Marsiske,⁶⁹ R. Messner,⁶⁹ D. R. Muller,⁶⁹ C. P. O’Grady,⁶⁹ V. E. Ozcan,⁶⁹ A. Perazzo,⁶⁹ M. Perl,⁶⁹ T. Pulliam,⁶⁹ B. N. Ratcliff,⁶⁹ A. Roodman,⁶⁹ A. A. Salnikov,⁶⁹ R. H. Schindler,⁶⁹ J. Schwiening,⁶⁹ A. Snyder,⁶⁹ J. Stelzer,⁶⁹ D. Su,⁶⁹ M. K. Sullivan,⁶⁹ K. Suzuki,⁶⁹ S. K. Swain,⁶⁹ J. M. Thompson,⁶⁹ J. Va’vra,⁶⁹ N. van Bakel,⁶⁹ M. Weaver,⁶⁹ A. J. R. Weinstein,⁶⁹ W. J. Wisniewski,⁶⁹ M. Wittgen,⁶⁹ D. H. Wright,⁶⁹ A. K. Yarritu,⁶⁹ K. Yi,⁶⁹ C. C. Young,⁶⁹ P. R. Burchat,⁷⁰ A. J. Edwards,⁷⁰ S. A. Majewski,⁷⁰ B. A. Petersen,⁷⁰ C. Roat,⁷⁰ L. Wilden,⁷⁰ S. Ahmed,⁷¹ M. S. Alam,⁷¹ R. Bula,⁷¹ J. A. Ernst,⁷¹ V. Jain,⁷¹ B. Pan,⁷¹ M. A. Saeed,⁷¹ F. R. Wappler,⁷¹ S. B. Zain,⁷¹ W. Bugg,⁷² M. Krishnamurthy,⁷² S. M. Spanier,⁷² R. Eckmann,⁷³ J. L. Ritchie,⁷³ A. Satpathy,⁷³ C. J. Schilling,⁷³ R. F. Schwitters,⁷³ J. M. Izen,⁷⁴ X. C. Lou,⁷⁴ S. Ye,⁷⁴ F. Bianchi,⁷⁵ F. Gallo,⁷⁵ D. Gamba,⁷⁵ M. Bomben,⁷⁶ L. Bosisio,⁷⁶ C. Cartaro,⁷⁶ F. Cossutti,⁷⁶ G. Della Ricca,⁷⁶ S. Dittongo,⁷⁶ L. Lancieri,⁷⁶ L. Vitale,⁷⁶ V. Azzolini,⁷⁷ N. Lopez-March,⁷⁷ F. Martinez-Vidal,⁷⁷ Sw. Banerjee,⁷⁸ B. Bhuyan,⁷⁸ C. M. Brown,⁷⁸ D. Fortin,⁷⁸ K. Hamano,⁷⁸ R. Kowalewski,⁷⁸ I. M. Nugent,⁷⁸ J. M. Roney,⁷⁸ R. J. Sobie,⁷⁸ J. J. Back,⁷⁹ P. F. Harrison,⁷⁹ T. E. Latham,⁷⁹ G. B. Mohanty,⁷⁹ M. Pappagallo,⁷⁹ H. R. Band,⁸⁰ X. Chen,⁸⁰ B. Cheng,⁸⁰ S. Dasu,⁸⁰ M. Datta,⁸⁰ K. T. Flood,⁸⁰ J. J. Hollar,⁸⁰ P. E. Kutter,⁸⁰ B. Mellado,⁸⁰ A. Mihalyi,⁸⁰ Y. Pan,⁸⁰ M. Pierini,⁸⁰ R. Prepost,⁸⁰ S. L. Wu,⁸⁰ Z. Yu,⁸⁰ and H. Neal⁸¹

(The BABAR Collaboration)

¹Laboratoire de Physique des Particules, IN2P3/CNRS et Université de Savoie, F-74941 Annecy-Le-Vieux, France

²Universitat de Barcelona, Facultat de Física, Departament ECM, E-08028 Barcelona, Spain

³Università di Bari, Dipartimento di Fisica and INFN, I-70126 Bari, Italy

⁴Institute of High Energy Physics, Beijing 100039, China

⁵University of Bergen, Institute of Physics, N-5007 Bergen, Norway

⁶Lawrence Berkeley National Laboratory and University of California, Berkeley, California 94720, USA

⁷University of Birmingham, Birmingham, B15 2TT, United Kingdom

⁸Ruhr Universität Bochum, Institut für Experimentalphysik 1, D-44780 Bochum, Germany

⁹University of Bristol, Bristol BS8 1TL, United Kingdom

¹⁰University of British Columbia, Vancouver, British Columbia, Canada V6T 1Z1

¹¹Brunel University, Uxbridge, Middlesex UB8 3PH, United Kingdom

¹²Budker Institute of Nuclear Physics, Novosibirsk 630090, Russia

¹³University of California at Irvine, Irvine, California 92697, USA

¹⁴University of California at Los Angeles, Los Angeles, California 90024, USA

¹⁵University of California at Riverside, Riverside, California 92521, USA

¹⁶University of California at San Diego, La Jolla, California 92093, USA

¹⁷University of California at Santa Barbara, Santa Barbara, California 93106, USA

¹⁸University of California at Santa Cruz, Institute for Particle Physics, Santa Cruz, California 95064, USA

¹⁹California Institute of Technology, Pasadena, California 91125, USA

²⁰University of Cincinnati, Cincinnati, Ohio 45221, USA

- ²¹ University of Colorado, Boulder, Colorado 80309, USA
- ²² Colorado State University, Fort Collins, Colorado 80523, USA
- ²³ Universität Dortmund, Institut für Physik, D-44221 Dortmund, Germany
- ²⁴ Technische Universität Dresden, Institut für Kern- und Teilchenphysik, D-01062 Dresden, Germany
- ²⁵ Laboratoire Leprince-Ringuet, CNRS/IN2P3, Ecole Polytechnique, F-91128 Palaiseau, France
- ²⁶ University of Edinburgh, Edinburgh EH9 3JZ, United Kingdom
- ²⁷ Università di Ferrara, Dipartimento di Fisica and INFN, I-44100 Ferrara, Italy
- ²⁸ Laboratori Nazionali di Frascati dell'INFN, I-00044 Frascati, Italy
- ²⁹ Università di Genova, Dipartimento di Fisica and INFN, I-16146 Genova, Italy
- ³⁰ Harvard University, Cambridge, Massachusetts 02138, USA
- ³¹ Universität Heidelberg, Physikalisches Institut, Philosophenweg 12, D-69120 Heidelberg, Germany
- ³² Imperial College London, London, SW7 2AZ, United Kingdom
- ³³ University of Iowa, Iowa City, Iowa 52242, USA
- ³⁴ Iowa State University, Ames, Iowa 50011-3160, USA
- ³⁵ Johns Hopkins University, Baltimore, Maryland 21218, USA
- ³⁶ Universität Karlsruhe, Institut für Experimentelle Kernphysik, D-76021 Karlsruhe, Germany
- ³⁷ Laboratoire de l'Accélérateur Linéaire, IN2P3/CNRS et Université Paris-Sud 11, Centre Scientifique d'Orsay, B.P. 34, F-91898 ORSAY Cedex, France
- ³⁸ Lawrence Livermore National Laboratory, Livermore, California 94550, USA
- ³⁹ University of Liverpool, Liverpool L69 7ZE, United Kingdom
- ⁴⁰ Queen Mary, University of London, E1 4NS, United Kingdom
- ⁴¹ University of London, Royal Holloway and Bedford New College, Egham, Surrey TW20 0EX, United Kingdom
- ⁴² University of Louisville, Louisville, Kentucky 40292, USA
- ⁴³ University of Manchester, Manchester M13 9PL, United Kingdom
- ⁴⁴ University of Maryland, College Park, Maryland 20742, USA
- ⁴⁵ University of Massachusetts, Amherst, Massachusetts 01003, USA
- ⁴⁶ Massachusetts Institute of Technology, Laboratory for Nuclear Science, Cambridge, Massachusetts 02139, USA
- ⁴⁷ McGill University, Montréal, Québec, Canada H3A 2T8
- ⁴⁸ Università di Milano, Dipartimento di Fisica and INFN, I-20133 Milano, Italy
- ⁴⁹ University of Mississippi, University, Mississippi 38677, USA
- ⁵⁰ Université de Montréal, Physique des Particules, Montréal, Québec, Canada H3C 3J7
- ⁵¹ Mount Holyoke College, South Hadley, Massachusetts 01075, USA
- ⁵² Università di Napoli Federico II, Dipartimento di Scienze Fisiche and INFN, I-80126, Napoli, Italy
- ⁵³ NIKHEF, National Institute for Nuclear Physics and High Energy Physics, NL-1009 DB Amsterdam, The Netherlands
- ⁵⁴ University of Notre Dame, Notre Dame, Indiana 46556, USA
- ⁵⁵ Ohio State University, Columbus, Ohio 43210, USA
- ⁵⁶ University of Oregon, Eugene, Oregon 97403, USA
- ⁵⁷ Università di Padova, Dipartimento di Fisica and INFN, I-35131 Padova, Italy
- ⁵⁸ Laboratoire de Physique Nucléaire et de Hautes Energies, IN2P3/CNRS, Université Pierre et Marie Curie-Paris6, Université Denis Diderot-Paris7, F-75252 Paris, France
- ⁵⁹ University of Pennsylvania, Philadelphia, Pennsylvania 19104, USA
- ⁶⁰ Università di Perugia, Dipartimento di Fisica and INFN, I-06100 Perugia, Italy
- ⁶¹ Università di Pisa, Dipartimento di Fisica, Scuola Normale Superiore and INFN, I-56127 Pisa, Italy
- ⁶² Prairie View A&M University, Prairie View, Texas 77446, USA
- ⁶³ Princeton University, Princeton, New Jersey 08544, USA
- ⁶⁴ Università di Roma La Sapienza, Dipartimento di Fisica and INFN, I-00185 Roma, Italy
- ⁶⁵ Universität Rostock, D-18051 Rostock, Germany
- ⁶⁶ Rutherford Appleton Laboratory, Chilton, Didcot, Oxon, OX11 0QX, United Kingdom
- ⁶⁷ DSM/Dapnia, CEA/Saclay, F-91191 Gif-sur-Yvette, France
- ⁶⁸ University of South Carolina, Columbia, South Carolina 29208, USA
- ⁶⁹ Stanford Linear Accelerator Center, Stanford, California 94309, USA
- ⁷⁰ Stanford University, Stanford, California 94305-4060, USA
- ⁷¹ State University of New York, Albany, New York 12222, USA
- ⁷² University of Tennessee, Knoxville, Tennessee 37996, USA
- ⁷³ University of Texas at Austin, Austin, Texas 78712, USA
- ⁷⁴ University of Texas at Dallas, Richardson, Texas 75083, USA
- ⁷⁵ Università di Torino, Dipartimento di Fisica Sperimentale and INFN, I-10125 Torino, Italy
- ⁷⁶ Università di Trieste, Dipartimento di Fisica and INFN, I-34127 Trieste, Italy
- ⁷⁷ IFIC, Universitat de Valencia-CSIC, E-46071 Valencia, Spain
- ⁷⁸ University of Victoria, Victoria, British Columbia, Canada V8W 3P6
- ⁷⁹ Department of Physics, University of Warwick, Coventry CV4 7AL, United Kingdom
- ⁸⁰ University of Wisconsin, Madison, Wisconsin 53706, USA
- ⁸¹ Yale University, New Haven, Connecticut 06511, USA

(Dated: October 6, 2006)

We study the initial-state-radiation processes $e^+e^- \rightarrow K^+K^-\pi^+\pi^-\gamma$ and $e^+e^- \rightarrow K^+K^-\pi^0\pi^0\gamma$ using an integrated luminosity of 232 fb^{-1} collected at the $\Upsilon(4S)$ mass with the *BABAR* detector at SLAC. Even though these reactions are dominated by intermediate states with excited kaons, we are able to study for the first time the cross section for $e^+e^- \rightarrow \phi(1020)f_0(980)$ as a function of center-of-mass energy. We observe a structure near threshold consistent with a 1^{--} resonance with mass $m = 2.175 \pm 0.010 \pm 0.015 \text{ GeV}/c^2$ and width $\Gamma = 58 \pm 16 \pm 20 \text{ MeV}$. We observe no $Y(4260)$ signal and set a limit of $\mathcal{B}_{Y \rightarrow \phi\pi^+\pi^-} \cdot \Gamma_{ee}^Y < 0.4 \text{ eV}$ (90% confidence level), which excludes some models.

PACS numbers: 13.66.Bc, 14.40.Cs, 13.25.Gv, 13.25.Jx, 13.20.Jf

The nature of the $Y(4260)$ resonance, which *BABAR* recently discovered [1] through its production via initial state radiation (ISR) in e^+e^- annihilations and its decay into $J/\psi\pi^+\pi^-$, remains unclear. It is well above threshold for the $D^{(*)}\overline{D}^{(*)}$ decays expected for a wide charmonium state, but no peak is observed in the total cross section $e^+e^- \rightarrow \text{hadrons}$ in this mass region. Some models [2] predict a large branching fraction for $Y(4260)$ into $\phi\pi\pi$. Moreover, the rich spectroscopy of the $J/\psi\pi\pi$ final state motivates a thorough investigation of the analogous $\phi\pi\pi$ state.

In this paper we update our previous analysis with ISR of $e^+e^- \rightarrow K^+K^-\pi^+\pi^-$ [3]. We include more data and relax the selection criteria, resulting in a fivefold increase in the number of selected events. We obtain an improved $e^+e^- \rightarrow K^+K^-\pi^+\pi^-$ cross section measurement over a wide range of effective e^+e^- center-of-mass (C.M.) energies, and perform the first studies of the $\phi\pi^+\pi^-$, $f_0(980)K^+K^-$ and ϕf_0 intermediate states. We also present the first measurements of the $e^+e^- \rightarrow K^+K^-\pi^0\pi^0$ cross section and its ϕf_0 component.

We use data corresponding to an integrated luminosity of 232 fb^{-1} recorded by the *BABAR* detector [4] on and off the $\Upsilon(4S)$ resonance. Charged-particle tracking is provided by a five-layer silicon vertex tracker (SVT) and a 40-layer drift chamber (DCH) in a 1.5 T axial magnetic field. Photon and electron energies are measured in a CsI(Tl) electromagnetic calorimeter (EMC). Charged particles are identified by specific ionization in the SVT and DCH, and an internally reflecting ring-imaging Cherenkov detector (DIRC).

We use a simulation package developed for radiative processes that generates hadronic final states following Ref. [5], multiple soft photons from the initial-state using a structure-function technique [6, 7], and photons from the final-state particles using PHOTOS [8]. We generate $K^+K^-\pi\pi$ final states both according to phase space and with a model that includes the $\phi(1020) \rightarrow K^+K^-$ and $f_0(980) \rightarrow \pi\pi$ channels. We pass the events through a detector simulation [9], and reconstruct them in the same way as we do the data. We generate a number of backgrounds with this package, including the ISR processes $e^+e^- \rightarrow \pi^+\pi^-\pi^+\pi^-\gamma$, $\pi^+\pi^-\pi^0\pi^0\gamma$, $\phi\eta\gamma$, $\phi\pi^0\gamma$ and $\pi^+\pi^-\pi^0\gamma$, and we also study $e^+e^- \rightarrow q\bar{q}$ events generated

by JETSET [10], $e^+e^- \rightarrow \tau^+\tau^-$ by KORALB [11], and $\Upsilon(4S)$ decays using our own generator [12].

The initial selection of events with a high-energy photon recoiling against a set of charged particles and photons is described in Refs. [3, 13]. Here we accept all charged tracks that extrapolate to the interaction region, and photon candidates with an EMC energy greater than 30 MeV. The reconstructed vertex of the set of charged tracks is used as the point of origin for all photons.

For each four-track event with one or two identified K^\pm , we perform a set of three-constraint kinematic fits (see Ref. [13]). We assume the photon with the highest C.M. energy to be from ISR, and the fits use its direction, along with the four-momenta and covariance matrices of the initial e^+e^- and the reconstructed tracks. A fit using the $\pi^+\pi^-\pi^+\pi^-$ hypothesis returns a $\chi_{4\pi}^2$. If the event contains an identified K^+ and K^- , we fit to the $K^+K^-\pi^+\pi^-$ hypothesis and require $\chi_{KK\pi^+\pi^-}^2 < 30$. For events with one identified kaon, we perform fits with each of the two oppositely charged tracks given the kaon hypothesis, and the combination with the lowest $\chi_{KK\pi^+\pi^-}^2$ is retained if it is lower than 30 and $\chi_{4\pi}^2 > \chi_{KK\pi^+\pi^-}^2$.

For the events with two tracks, both identified as charged kaons, and five or more photon candidates, all non-ISR photons are paired, and combinations lying within 35 MeV/ c^2 of the π^0 mass are considered π^0 candidates. We perform a six-constraint fit to each set of two non-overlapping π^0 candidates plus the ISR photon and the K^+ and K^- tracks, and the combination with the lowest $\chi_{KK\pi^0\pi^0}^2$ is retained if $\chi_{KK\pi^0\pi^0}^2 < 50$. To suppress ISR $K^+K^-\pi^0$ and $K^+K^-\eta$ events, in which photons from an energetic π^0 or η combine with soft background clusters to form two π^0 candidates, we reject events with large differences between the two photon energies in both π^0 candidates. The fitted three-momenta for each charged track and photon are used in further kinematical calculations.

We consider three types of backgrounds. The first, which peaks at low values of χ^2 , is due to non-ISR events, and is dominated by $e^+e^- \rightarrow q\bar{q}$ events with a hard π^0 producing a fake ISR photon. To evaluate this background, we use simulated mass and χ^2 distributions normalized to data events in which the ISR photon combines with another cluster to form a π^0 can-

didate. The second type of background, due to ISR $e^+e^- \rightarrow \pi^+\pi^-\pi\pi$ events with misidentified π^\pm , also contributes at low χ^2 values. We derive reliable estimates of their contributions from the known cross sections [3]. The third type of background comprises all remaining background sources and is estimated from the control regions $30 < \chi_{KK\pi^+\pi^-}^2 < 60$ and $50 < \chi_{KK\pi^0\pi^0}^2 < 100$, as detailed in Refs. [3, 13]. We subtract these backgrounds, about 8-10% (15-20%) total contribution, from the selected $K^+K^-\pi^+\pi^-$ ($K^+K^-\pi^0\pi^0$) events.

We measure the track-finding efficiency from the data, and measure the kaon identification efficiency from a clean sample of ISR $e^+e^- \rightarrow \phi \rightarrow K^+K^-$ events to a precision of 2.0%, a fourfold improvement over our previous result [3]. The π^0 reconstruction efficiency is determined from ISR $e^+e^- \rightarrow \omega\pi^0\gamma \rightarrow \pi^+\pi^-\pi^0\pi^0\gamma$ events and the method described in Ref. [13]. The above procedures allow us to correct the efficiency obtained from the MC simulation. In Fig. 1 we show the cross sections for the two processes, calculated by dividing the background-subtracted yield in each bin by the efficiency and the ISR luminosity [3]. The errors are statistical only. The $e^+e^- \rightarrow K^+K^-\pi^+\pi^-$ cross section (Fig. 1a) is consistent with both the direct measurement by DM1 [14] and our previous measurement [3], but is far more precise. In addition to the sharp J/ψ peak, wider structures are visible near 1.8 GeV, 2.2 GeV and possibly 2.4 GeV. The $e^+e^- \rightarrow K^+K^-\pi^0\pi^0$ cross section (Fig. 1b) shows the same general features, including a J/ψ peak and a steep drop around 2.2 GeV. The total systematic uncertainty in the $K^+K^-\pi^+\pi^-$ ($\pi^0\pi^0$) cross section ranges from 7% (10%) at threshold to 9% (15%) at high $E_{C.M.}$.

As seen previously [3], there is a rich substructure in the $e^+e^- \rightarrow K^+K^-\pi^+\pi^-$ process, dominated by the $K^{*0}(892)K\pi$ intermediate state, but with large signals from the $K_1(1270)$, $K_2^{*0}(1430)$ and $K_1(1400)$ resonances. The $e^+e^- \rightarrow K^+K^-\pi^0\pi^0$ process is also dominated by the $K^{*\pm}(892)K^\mp\pi^0$ intermediate state. Understanding these contributions via a partial wave analysis is outside the scope of this paper.

Here we concentrate on events with an intermediate $\phi(1020)$ and/or $f_0(980)$ state. Figure 2 shows scatter plots of $m(\pi^+\pi^-)$ or $m(\pi^0\pi^0)$ versus $m(K^+K^-)$ for the selected events (including backgrounds) in the data. A $\phi \rightarrow K^+K^-$ band is visible in both cases, as well as a concentration of events indicating correlated production of ϕ and f_0 . A horizontal $\rho(770)$ band is visible for the charged mode only, and is due to $K_1 \rightarrow K\rho$ decays. Most of the K^* intermediate states are outside the bounds of these plots. Selecting ϕ events with $|m(K^+K^-) - 1020 \text{ MeV}/c^2| < 10 \text{ MeV}/c^2$, and subtracting events with $10 < |m(K^+K^-) - 1020 \text{ MeV}/c^2| < 20 \text{ MeV}/c^2$ (see Figs. 3a,c) and MC simulated backgrounds, we obtain the ϕ -associated $m(\pi\pi)$ distributions shown in Figs. 3b,d. Clear $f_0(980)$ signals are visible in both cases, and there is an indication of $f_2(1270) \rightarrow \pi^+\pi^-$.

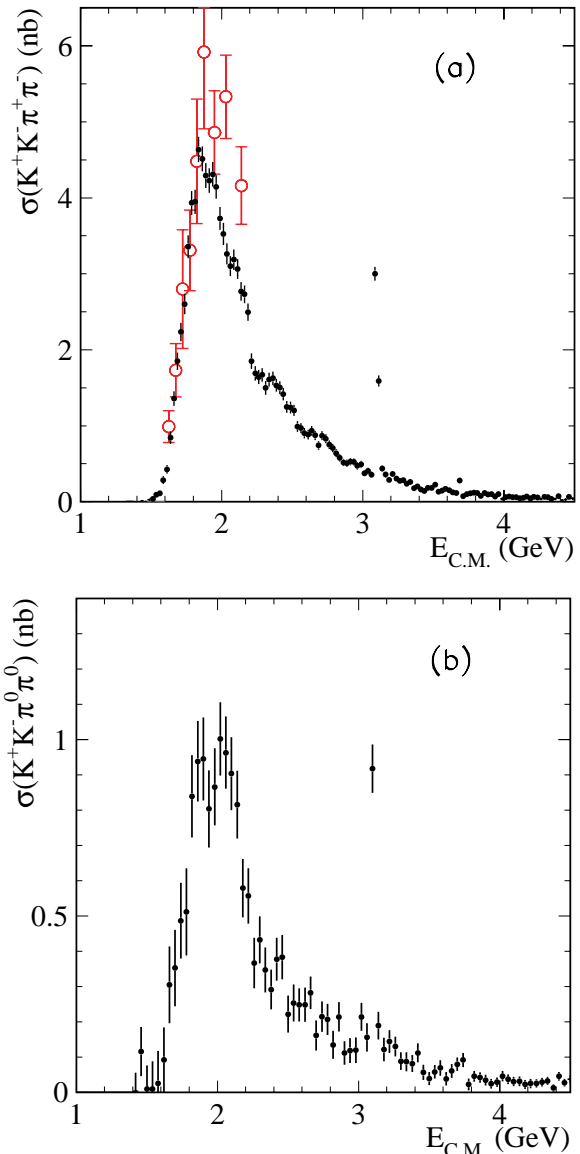


FIG. 1: The a) $e^+e^- \rightarrow K^+K^-\pi^+\pi^-$ and b) $e^+e^- \rightarrow K^+K^-\pi^0\pi^0$ cross sections as a function of e^+e^- C.M. energy. The direct measurements by DM1 [14] are shown for comparison as open circles. Only statistical errors are shown.

The histogram in Fig. 3b is the result of a simulation that includes $f_0(600)$, $f_0(980)$ and a small fraction of $f_2(1270)$ resonances and describes the general features of the distribution. The curve in Fig. 3d shows a fit of two Breit-Wigner functions corresponding to the $f_0(600)$ and $f_0(980)$ with the relative phase set to π ; events with $m(\pi^0\pi^0) < 0.45 \text{ GeV}/c^2$ are dominated by background-subtraction uncertainties and not used in the fit. The fitted f_0 parameters are consistent with PDG [15] values. Figure 4 shows the $m(K^+K^-\pi\pi)$ distributions in the charmonium region for events with $m(K^+K^-)$ in the ϕ signal and sideband regions. There is a strong J/ψ signal in both samples; from the signal-sideband differences of 103 ± 12 and 23 ± 6 events, we calculate

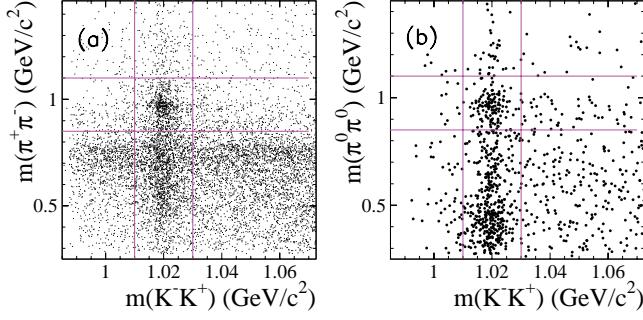


FIG. 2: The scatter plots of the reconstructed a) $m(\pi^+\pi^-)$ and b) $m(\pi^0\pi^0)$ versus $m(K^+K^-)$ for selected events in the data. The vertical (horizontal) lines bound a ϕ ($f_0(980)$) signal region.

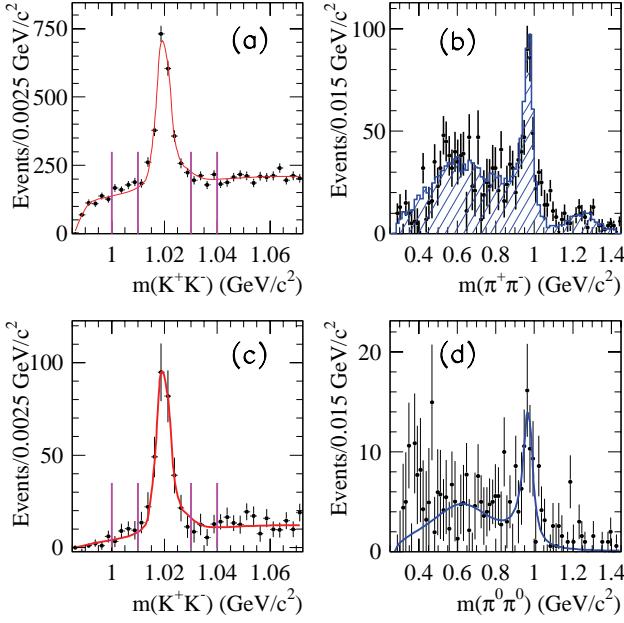


FIG. 3: The $m(K^+K^-)$ projections for the a) $K^+K^-\pi^+\pi^-$ and c) $K^+K^-\pi^0\pi^0$ candidates in the data. The vertical lines delimit ϕ signal and sideband regions. b,d) $m(\pi\pi)$ distribution for events in the ϕ signal region of (a,c) minus that for events in the sidebands. The curves (histogram) represent the results of the fits (simulation) described in the text.

$\mathcal{B}_{J/\psi \rightarrow \phi\pi^+\pi^-} \cdot \Gamma_{ee}^{J/\psi} \cdot \mathcal{B}_{\phi \rightarrow K^+K^-} = (2.61 \pm 0.30 \pm 0.18)$ eV and the first measurement of

$\mathcal{B}_{J/\psi \rightarrow \phi\pi^0\pi^0} \cdot \Gamma_{ee}^{J/\psi} \cdot \mathcal{B}_{\phi \rightarrow K^+K^-} = (1.54 \pm 0.40 \pm 0.16)$ eV. We also observe 10 ± 4 $\psi(2S) \rightarrow \phi\pi^+\pi^-$ decays, from which we determine

$\mathcal{B}_{\psi(2S) \rightarrow \phi\pi^+\pi^-} \cdot \Gamma_{ee}^{\psi(2S)} \cdot \mathcal{B}_{\phi \rightarrow K^+K^-} = (0.28 \pm 0.11 \pm 0.02)$ eV.

There is no signal for $Y(4260) \rightarrow \phi\pi^+\pi^-$. In the region $|m(\phi\pi^+\pi^-) - m(Y)| < 0.1$ GeV/ c^2 we find 10 events, and assuming a uniform distribution we estimate 9.2 background events from the 3.8–5.0 GeV/ c^2 region. This corresponds to upper limits of 5.0 events and

$$\mathcal{B}_{Y \rightarrow \phi\pi^+\pi^-} \cdot \Gamma_{ee}^Y < 0.4 \text{ eV}$$

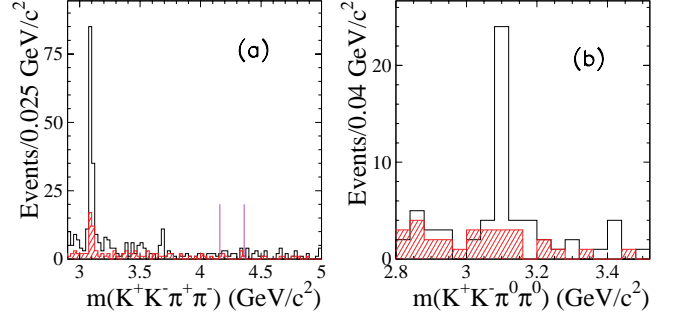


FIG. 4: The a) $m(K^+K^-\pi^+\pi^-)$ and b) $m(K^+K^-\pi^0\pi^0)$ distributions in the charmonium region for events in the ϕ signal (open histogram) and sideband (shaded histogram) regions. The vertical lines indicate the range used for the $Y(4260)$ search.

at the 90% confidence level, which is in agreement with the upper limit obtained by CLEO [16] and is well below our analogous measurement $\mathcal{B}_{Y \rightarrow J/\psi\pi^+\pi^-} \cdot \Gamma_{ee}^Y = (5.5 \pm 1.1^{+0.8}_{-0.7})$ eV [1]. This excludes models (e.g. [2]) in which these two $Y(4260)$ branching fractions are comparable.

We now consider the quasi-two-body intermediate state $\phi f_0(980)$. In each 25 MeV/ c^2 (40 MeV/ c^2) bin of $m(K^+K^-\pi\pi)$ we select $K^+K^-\pi^+\pi^-$ ($K^+K^-\pi^0\pi^0$) events with $m(\pi^+\pi^-)$ ($m(\pi^0\pi^0)$) in the 0.85–1.1 GeV/ c^2 region and fit their $m(K^+K^-)$ distribution to extract the number of events with a true ϕ . These are shown in Fig. 5 with about 700 events for the $K^+K^-\pi^+\pi^-$ channel and about 120 events for the $K^+K^-\pi^0\pi^0$ channel; there is a contribution of about 10% from $e^+e^- \rightarrow \phi\pi\pi$ events where the pion pair is not produced through the $f_0(980)$. Both distributions show the sharp rise from threshold as expected for a pair of relatively narrow resonances, and a slow, smooth decrease at high $E_{C.M.}$, with signals for J/ψ and $\psi(2S)$ in Fig. 5a. Both also show a resonance-like structure at about 2.15 GeV/ c^2 . There are no known meson resonances with $I=0$ near this mass.

Dividing by the efficiency, ISR luminosity, $\mathcal{B}_{\phi \rightarrow K^+K^-} = 0.491$ [15], and $\mathcal{B}_{f_0 \rightarrow \pi^+\pi^- (\pi^0\pi^0)} = 2/3(1/3)$, we obtain the two consistent measurements of the $e^+e^- \rightarrow \phi f_0$ cross section shown in Fig. 6 (including about 10% $\phi\pi\pi$ contribution). We use the following function of $s = E_{C.M.}^2$:

$$\sigma(s) = \frac{P(s)}{P(m_x^2)} \cdot \left| A_{nr} e^{-i\psi_x} + \frac{\sqrt{\sigma_0} m_x \Gamma_x}{m_x^2 - s - i\sqrt{s}\Gamma_x} \right|^2, \quad (1)$$

$$A_{nr}(s) = N_{nr} \cdot (1 - e^{-(\mu/a_1)^4}) \cdot (1 + a_2\mu + a_3\mu^2), \quad (2)$$

$$\mu = \sqrt{s} - m_0, \quad P(s) = \sqrt{1 - m_0^2/s}$$

where N_{nr} normalizes the amplitude of the non-resonant spectrum, σ_0 is a peak cross section for the hypothesized resonance, and m_x , Γ_x and $-\psi_x$ are the mass, total width and relative phase of the non-resonant amplitude to the standard Breit-Wigner amplitude. The factor $P(s)$ gives a good approximation of the two-body phase space factor

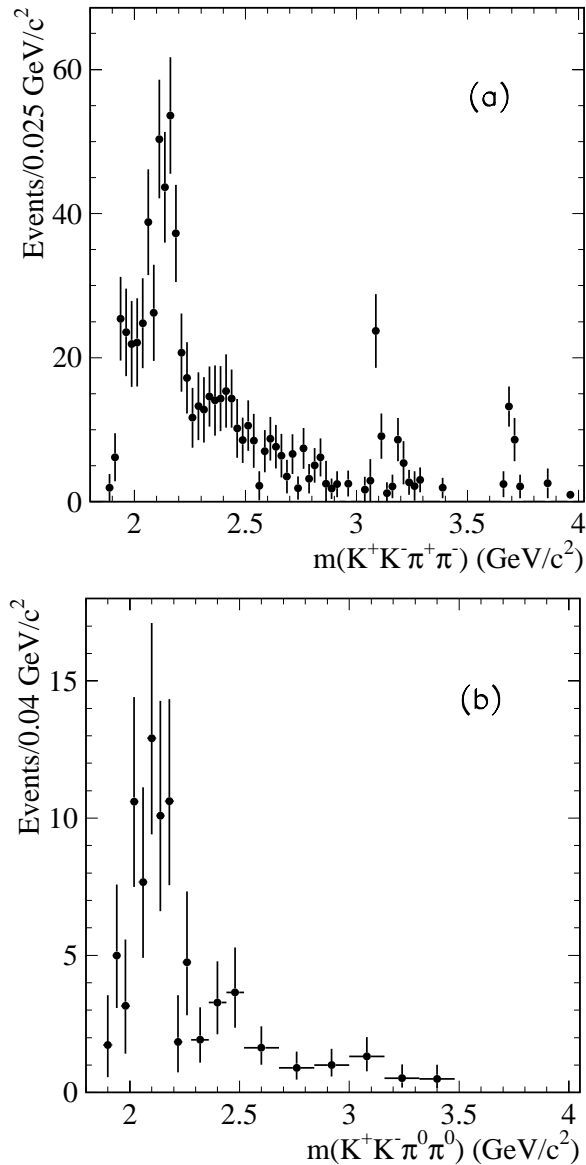


FIG. 5: The number of a) $e^+e^- \rightarrow \phi f_0 \rightarrow K^+K^-\pi^+\pi^-$ and b) $e^+e^- \rightarrow \phi f_0 \rightarrow K^+K^-\pi^0\pi^0$ events vs. invariant mass extracted as described in the text. Some bins have been combined for clarity, as indicated by the horizontal error bars.

for particles with similar masses; both the $\phi(1020)$ and $f_0(980)$ have small but finite widths, and our selection cut of $m(\pi\pi) > 0.85$ GeV/c^2 defines an effective minimum mass, $m_0 = 1.8$ GeV/c^2 . The form of A_{nr} is determined from a simulation that takes the ϕ and $f_0(980)$ lineshapes into account. A very sharp exponential cutoff (parameter a_1) is needed to describe the simulation well, but does not affect the spectrum well above threshold. There is no theoretical prediction for the form at high s , other than that, in the absence of resonances, it should fall smoothly with increasing s . A second order polynomial (parameters a_2 and a_3) describes the simulation, so we fit Eq. 2 to the data, floating N_{nr} , a_1 , a_2 and a_3 . The result without a resonant component is shown as the dashed

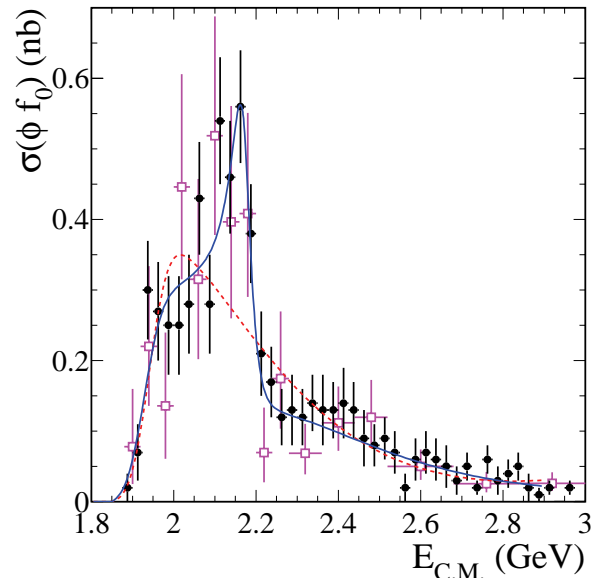


FIG. 6: The $e^+e^- \rightarrow \phi(1020)f_0(980)$ cross section, with about 10% of the $\phi\pi\pi$ contribution, obtained via ISR in the $K^+K^-\pi^+\pi^-$ (circles) and $K^+K^-\pi^0\pi^0$ (squares) final states. The curves represent results of the fits described in the text.

curve in Fig. 6. The $\chi_0^2 = 80.5/(56 - 5)$ has confidence level $P(\chi_0^2) = 0.0053$, and the fitted parameter values are close to those from the simulation; it is unlikely that a simple, smooth threshold curve can accommodate the data.

Including a single resonance (Eq. 1), we obtain a good fit with $\chi_x^2 = 37.6/(56 - 9)$ ($P(\chi_x^2) = 0.84$), shown as the solid line in Fig. 6. The fitted resonance parameter values are

$$\begin{aligned} \sigma_0 &= 0.13 \pm 0.04 \pm 0.02 \text{ nb}, \\ m_x &= 2.175 \pm 0.010 \pm 0.015 \text{ GeV}/c^2, \\ \Gamma_x &= 0.058 \pm 0.016 \pm 0.020 \text{ GeV}/c^2, \text{ and} \\ \psi_x &= -0.57 \pm 0.30 \pm 0.20 \text{ rad}. \end{aligned}$$

The first error is statistical and the second is systematic. Monte Carlo simulations show that the probability of such a signal arising by chance is less than 10^{-3} . The modestly negative value of ψ_x provides constructive interference below the resonance peak and destructive interference above it, in accord with the data. Variations in the resonance parameters are used to estimate the systematic errors. The fit of the mass spectra in Fig. 5a,b with Eq. 1 with normalization to the number of events under the Breit-Wigner curve gives 170 ± 63 and 31 ± 15 events for $\pi^+\pi^-$ and $\pi^0\pi^0$ respectively. Note that the observed structure is close to the $\Lambda\bar{\Lambda}$ production threshold at 2.23 GeV/c^2 and the opening of this channel may also contribute to the ϕf_0 cross section.

We perform a number of systematic checks. Treating selected $K^+K^-K^+K^-$ and $\pi^+\pi^-\pi\pi$ events as signal, we observe no structure. Selecting $K^*(892)K\pi$ events, which have little kinematic overlap with $\phi f_0(980)$, we see no structure. Excluding the dominant $K^*(892)K\pi$ intermediate states and selecting events with $m(\pi^+\pi^-)$ in the

range 0.6–0.85 GeV/ c^2 for the charged mode we observe structure at 2.15 GeV/ c^2 with a similar yield. Because of the many overlapping intermediate states we cannot perform a quantitative measurement. This will be the subject of future investigation. Events with no $f_0(980)$ candidate do not exhibit a structure in the $K^+K^-\pi^0\pi^0$ mode. We conclude that the new structure decays to $\phi f_0(980)$ with a relatively large branching fraction. We estimate

$$\mathcal{B}_{x \rightarrow \phi f_0} \cdot \Gamma_{ee}^x = \frac{\Gamma_x \sigma_0 m_x^2}{12\pi C} = (2.5 \pm 0.8 \pm 0.4) \text{ eV} ,$$

where we fit the product $\Gamma_x \sigma_0$ to reduce correlations, and the conversion constant $C = 0.389 \text{ mb (GeV}/c^2)^2$.

In summary, we present the most precise measurements of the cross sections for $e^+e^- \rightarrow K^+K^-\pi^+\pi^-$ and $e^+e^- \rightarrow K^+K^-\pi^0\pi^0$ from threshold to 4.5 GeV. In the $\phi\pi\pi$ channels we observe the J/ψ and $\psi(2S)$ but not the $Y(4260)$. In the ϕf_0 channel, we observe a new resonance-like structure, which might be interpreted as an $s\bar{s}$ analogue of the $Y(4260)$, or as an $s\bar{s}s\bar{s}$ state that decays predominantly to $\phi f_0(980)$.

We are grateful for the excellent luminosity and machine conditions provided by our PEP-II colleagues, and for the substantial dedicated effort from the computing organizations that support *BABAR*. The collaborating institutions wish to thank SLAC for its support and kind hospitality. This work is supported by DOE and NSF (USA), NSERC (Canada), IHEP (China), CEA and CNRS-IN2P3 (France), BMBF and DFG (Germany), INFN (Italy), FOM (The Netherlands), NFR (Norway), MIST (Russia), MEC (Spain), and PPARC (United Kingdom). Individuals have received support

from the Marie Curie EIF (European Union) and the A. P. Sloan Foundation.

-
- * Also with Università di Perugia, Dipartimento di Fisica, Perugia, Italy
 - † Also with Università della Basilicata, Potenza, Italy
 - [1] *BABAR* Collaboration, B. Aubert *et al.*, Phys. Rev. Lett. **95**, 142001 (2005).
 - [2] Shi-Lin Zhu, Phys. Lett. **B625**, 212 (2005).
 - [3] *BABAR* Collaboration, B. Aubert *et al.*, Phys. Rev. **D71**, 052001 (2005).
 - [4] *BABAR* Collaboration, B. Aubert *et al.*, Nucl. Instrum. Meth. **A479**, 1 (2002).
 - [5] H. Czyż and J. H. Kühn, Eur. Phys. J. **C18**, 497 (2001).
 - [6] A. B. Arbuzov *et al.*, J. High Energy Phys. **9710**, 001 (1997).
 - [7] M. Caffo, H. Czyż and E. Remiddi, Nuovo Cim. **A110**, 515 (1997); Phys. Lett. **B327**, 369 (1994).
 - [8] E. Barberio, B. van Eijk and Z. Was, Comput. Phys. Commun. **66**, 115 (1991).
 - [9] GEANT4 Collaboration, S. Agostinelli *et al.*, Nucl. Instrum. Methods Phys. Res., Sect. A **506**, 250 (2003).
 - [10] T. Sjöstrand, Comput. Phys. Commun. **82**, 74 (1994).
 - [11] S. Jadach and Z. Was, Comput. Phys. Commun. **85**, 453 (1995).
 - [12] D. J. Lange, Nucl. Instrum. Meth. **A462**, 152 (2001).
 - [13] *BABAR* Collaboration, B. Aubert *et al.*, Phys. Rev. **D73**, 052003 (2006).
 - [14] DM1 Collaboration, A. Cordier *et al.*, Phys. Lett. **B110**, 335 (1982).
 - [15] Review of Particle Physics, S. Eidelman *et al.*, Phys. Lett. **B592**, 1 (2004).
 - [16] CLEO Collaboration, T. E. Coan *et al.*, Phys. Rev. Lett. **96**, 162003 (2006).